Unusual Thermal Stability of RNA/[R_P-PS]-DNA/RNA Triplexes Containing a Homopurine DNA Strand

Piotr Guga,* Małgorzata Boczkowska,* Magdalena Janicka,* Anna Maciaszek,* Sławomir Kuberski,† and Wojciech J. Stec*

*Department of Bioorganic Chemistry, Centre of Molecular and Macromolecular Studies, Polish Academy of Sciences, Łódź, Poland; and †Faculty of Process and Environmental Engineering, Technical University of Łódź, Łódź, Poland

ABSTRACT Homopurine deoxyribonucleoside phosphorothioates, as short as hexanucleotides and possessing all internucleotide linkages of R_P configuration, form a triple helix with two RNA or 2′-OMe-RNA strands, with Watson-Crick and Hoogsteen complementarity. Melting temperature and fluorescence quenching experiments strongly suggest that the Hoogsteen RNA strand is parallel to the homopurine [R_P-PS]-oligomer. Remarkably, these triplexes are thermally more stable than complexes formed by unmodified homopurine DNA molecules of the same sequence. The triplexes formed by phosphorothioate DNA dodecamers containing 4–6 dG residues are thermally stable at pH 7.4, although their stability increases significantly at pH 5.3. FTIR measurements suggest participation of the C^2-carbonyl group of the pyrimidines in the stabilization of the triplex structure. Formation of triple-helix complexes with exogenously delivered PS-oligos may become useful for the reduction of RNA accessibility in vivo and, hence, selective suppression/inhibition of the translation process.

INTRODUCTION

Triple-helical forms of nucleic acids have been known since 1957 (1). In triplexes, the third strand binds either in a parallel or an antiparallel orientation with respect to the purine strand in the duplex, due to formation of Hoogsteen or reverse Hoogsteen hydrogen bonds, respectively (2). In principle, triplexes can be formed from different combinations of RNA and DNA strands, and the composition affects their stability (3–5). Pyrimidine RNA strands bind to DNA/DNA, RNA/RNA, and DNA/RNA duplexes, whereas pyrimidine DNA strands bind only to duplexes with a purine DNA strand. Oligonucleotide-directed triple-helix formation appears to be an important method for sequence-specific recognition of a double helix. This approach has been used for single site-specific cleavage of human chromosomal DNA (6) as well as for inhibition of transcription in vitro (7,8) and in vivo (9). Because natural oligodeoxyribonucleotides are easily degraded by nucleases, several modifications of the sugar-phosphate backbone have been introduced (10–13). Among these phosphorothioate analogs of DNA (PS-oligos) appear to be very important because of the close similarity of their properties to natural DNA and their enhanced stability against nucleolytic degradation. Usually, PS-oligos and complementary DNA and RNA strands form less stable duplexes (14,15). PS-oligos attracted a lot of attention as therapeutic agents in so-called antisense strategy. However, PS-oligos prepared by routine chemical methods consist of a mixture of diastereomers (16,17), whereas enzymatic synthesis, albeit feasible, provides PS-oligos of only R_P configuration (18). The oxathiaphospholane approach developed in this laboratory allows for preparation of PS-oligos with a predetermined sense of P-chirality (19,20) and has made possible a correlation of their stereochemistry with the thermal stability of complexes formed with complementary templates (14). It has also been found that stereochemistry of internucleotide bonds is critical for the ability of duplexes consisting of self-complementary [PS]-d$(CG)_4$ and [PS]-d$(GC)_4$ to exhibit a B-Z conformational change (21).

In principle, PS-oligos can form both parallel and antiparallel triplexes. In all cases except one, a PS-oligo binds in the major groove of a homopurine/homopyrimidine duplex (22–24) and the stability of the resulting triplexes is lower than that of the unmodified ones. It was also shown that homopurine phosphorothioate oligonucleotides inhibited transcription of the gene α1(I) of collagen by formation of a triplex with homopurine-homopyrimidine sequence of the DNA promotor localized at position from −200 to −171 from the point of the start of transcription (25). There is just one report of a parallel triplex with a stereoregular [R_P-PS]-poly-d(AG) as the central homopurine strand bound to two unmodified

Submitted October 12, 2006, and accepted for publication December 21, 2006.

Address reprint requests to Prof. Dr. Wojciech J. Stec, Tel.: 48-42-6819744; Fax: 48-42-6815483; E-mail: wjstec@bio.cbmm.lodz.pl.

Abbreviations used: T_m, melting temperature, the temperature in a thermal dissociation experiment at which 50% of given DNA molecules still form a complex and the other 50% have been separated; T_a, association temperature, the temperature in a thermal association experiment at which 50% of given DNA molecules have formed a complex and the other 50% remain separated; FTIR, Fourier transformation infrared spectroscopy; PS-oligos, phosphorothioate analogues of DNA; CPG, controlled pore glass; RP-HPLC, reversed phase–high performance liquid chromatography; MALDI-TOF, matrix assisted laser desorption ionization–time of flight; PAGE, polyacrylamide gel electrophoresis; in the compound labels: a), descriptors [R_P-PS], [S_P-PS], [Mix-PS] indicate phosphorothioate analogues of DNA possessing all phosphorus atoms of R_P, S_P, or randomal absolute configuration, respectively; b), a descriptor [PO] indicates a natural, nonmodified DNA molecule; c), the suffixes **W** and **H** indicate RNA strands complementary to the corresponding homopurine DNA strands in a Watson-Crick and Hoogsteen sense, respectively.

0006-3495/07/04/2507/09 $2.00

doi: 10.1529/biophysj.106.099283

homopyrimidine DNA strands. The thermal stability of this triplex was higher than that of the unmodified one (ΔT_m = 12°C) (26).

To date, PS-oligos were found to form the triplex structures only with two other DNA strands. In our studies of the stability of heteroduplexes formed by P-stereodefined PS-oligos with complementary RNA matrices, we have observed enhanced stability of a structure formed by [R_P-PS]-dA_{12} with U_{12} as compared to the complex formed by nonmodified dA_{12} (27). Our results on stoichiometry and thermal stability of complexes formed between other model [R_P-PS]-homopurine oligomers and RNA templates provide evidence for a parallel triplex structure RNA/[PS]-DNA/RNA, which to the best of our knowledge has not been reported in the literature previously.

MATERIALS AND METHODS

Tris(hydroxymethyl)aminomethane (Tris base) and sodium chloride (both of Aristar quality) were purchased from BDH Laboratory, Poole, UK. Magnesium chloride pro analysi was obtained from Merck, Darmstadt, Germany. For the titration of Tris base, hydrochloric acid (amino acid analysis grade reagent, Applied Biosystems, Foster City, CA) was used. Sodium acetate buffer of 0.1 M concentration (pH 5.3) was obtained by dilution of concentrated sodium acetate buffer (3 M, pH 5.5) supplied by Applied Biosystems. All absorption measurements and ultraviolet (UV) monitored melting experiments were carried out in a 1-cm pathlength cell with either a UV/VIS 916 or a CINTRA 40 spectrophotometer (GBC, Dandenong, Australia), both equipped with a Peltier thermocell.

Chemical synthesis of oligonucleotides

The synthesis of P-stereodefined [PS]-oligonucleotides was performed manually. The first nucleoside units were anchored to the solid support by a sarcosinyl linker (28). Appropriately protected deoxyguanosyl, deoxyadenosyl, and (7-deaza)-deoxyadenosyl monomers possessing 3′-*O*-(2-thio-′′spiro′′-4,4-pentamethylene-1,3,2-oxathiaphospholane) moiety were synthesized and separated chromatographically into pure diastereomers. The protocol for the synthesis has been previously described (19,20).

The synthesis of unmodified DNA, [Mix-PS]-DNA, RNA and 2′-OMe-RNA oligonucleotides was performed on an ABI 380B DNA or ABI 394 DNA/RNA synthesizers (Applied Biosystems) at a 1 μmol scale using standard phosphoramidite DNA and RNA protocols.

The fluorescently labeled 2′-OMe-RNA oligomers were synthesized using the standard phosphoramidite method. For the synthesis of the oligonucleotides carrying 6-carboxyfluorescein at the 3′-end or 5′-end, appropriate CPG support or phosphoramidite reagent were used (CPG, Lincoln Park, NJ).

The stereodefined oligomer [R_P-PS]-d(GAGGAAAGAGAG), to be labeled at the 5′-end with a static ''BHQ-1'' quencher (the dye has broad strong absorbance centered around λ_{max} = 534 nm) to form [R_P-PS]-BHQ_{PS}d(GAGGAAAGAGAG) (**7B**), was synthesized manually on the solid support (vide supra), then detritylated and reacted with a ''BHQ-1'' phosphoramidite (4′-(2-nitro-4-toluyldiazo)-2′-methoxy-5′-methyl-azobenzene-4′′-(*N*-ethyl)-*N*-ethyl-2-cyanoethyl-(*N*,*N*-diisopropyl)-phosphoramidite; Glen Research, Sterling, VA) in the presence of 1*H*-tetrazole, followed by sulfurization. Therefore, the phosphorothioate linkage of random configuration was formed between the quencher and the 5′-dG residue.

All synthesized oligomers were purified by two-step RP-HPLC (DMT-on and DMT-off), and their purity was assessed by MALDI-TOF mass spectrometry (a Voyager-Elite instrument operating in the reflector mode with detection of negative ions; PerSeptive Biosystems, Framingham, MA) and polyacrylamide gel electrophoresis.

Sample preparation and melting profile recording

The concentration of oligomers was determined spectrophotometrically by UV absorbance at their λ_{max} in water, using the extinction coefficients calculated by the standard method (29). The samples were then lyophilized and redissolved in 10 mM Tris-HCl, 100 mM NaCl, 10 mM $MgCl_2$ buffer (pH 7.4), or 100 mM sodium acetate, 10 mM $MgCl_2$ (pH 5.3). Melting profiles were measured at a total oligonucleotide concentration of 4.0 μM with a temperature gradient of 0.2°C/min. The melting temperatures were calculated using the first order derivative method.

Mixing curves

The oligonucleotide solutions were prepared in the following way: to the six samples of an homopurine oligodeoxyribonucleotide or its phosphorothioate analog (0.2 OD units, 154 OD/μmol) 0.07, 0.13, 0.20, 0.26, 0.33, 0.39 OD units of homopyrimidine RNA or DNA oligonucleotide (102 OD/μmol) were added to the final molar ratios of 67:33, 50:50, 39:61, 34:66, 28:72, and 25:75, respectively. The seventh sample contained only the homopurine DNA strand. All samples were dissolved in a 10 mM Tris-HCl, 100 mM NaCl, 10 mM $MgCl_2$ buffer (pH 7.4) and equilibrated at 10°C for 2 h. The final absorptions were measured at λ = 260nm (at 10°C and/or 25°C) and normalized by dividing over the calculated total absorption of all strands present in the samples.

Measurements of fluorescence

Fluorescence quenching measurements were made in cuvettes with a 1-cm pathlength using a Cary Eclipse spectrophotometer (Varian Australia, Clayton South, Australia) with a thermostatting Peltier element accessory. The samples at concentration of 2 μM were dissolved in a buffer containing 10 mM Tris-HCl, 100 mM NaCl, 10 mM $MgCl_2$ buffer (pH 7.4). The excitation and emission slits were set at 5 or 10 nm.

FTIR spectra recording

The spectra were recorded on an FTIR-610 (MultiScan) spectrofotometer (Jasco Instruments, Tokyo, Japan) within a range 5000–500 cm^{-1} with a resolution of 2 cm^{-1}. Thirty scans were collected for each spectrum and the spectra were smoothed with 21-point Savitzky-Golay filter algorithm without baseline correction.

RESULTS AND DISCUSSION

Evidences for triplex formation

As mentioned in the introduction, the complex formed by [R_P-PS]-dA_{12} ([R_P-PS]-**1**) and complementary oligoribonucleotide U_{12} (**1W**) is thermally more stable than the complex formed by nonmodified dA_{12} with the same template (T_m = 37 vs. 23°C, respectively; under the same conditions, Table 1). The UV monitored mixing experiments at 10 and 25°C at neutrality (pH 7.4), showed the lowest normalized absorption at [R_P-PS]-**1/1W** ratio 1:2, what indicates the formation of a triplex structure (Fig. 1 *a*). The nondenaturing PAGE analysis for [R_P-PS]-dA_{12} mixed with the U_{12} at 2:1–1:3 molar ratio showed the disappearance of the band of [R_P-PS]-dA_{12} at the ratio PS-DNA/RNA between 1:2 and 1:2.5 (Fig. 2). As the nitrogen atom at position 7 of adenine plays a crucial role for association of the third strand, we have synthesized [R_P-PS]-(7-deaza-$dA)_{12}$ and found that its

TABLE 1 Melting (T_m) and association (T_a) temperatures for complexes [PO]-DNA/RNA and [PS]-DNA/RNA at molar ratio 1:1 and 1:2

Sequences	Form of DNA or PS-DNA	Molar ratio 1:1		Molar ratio 1:2	
		T_m	T_a	T_m	T_a
1 5′-d(AAAAAAAAAAAA)	[PO]	23 (33)	23 (34)	23 (41)	23 (41)
1W 3′-r(UUUUUUUUUUUU)	[R_P]	37 (46)	33 (46)	37 (53)	35 (53)
	[S_P]	18	18	18	18
2 5′-d(GAGAAAAAAGAG)	[PO]	26	26	26	26
2W 3′-r(CUCUUUUUUCUC)	[R_P]	54	35	54	36
	[S_P]	16	16	16	16
3 5′-d(GAGAGAAAAGAG)	[PO]	33	33	33 (38)	33 (38)
3W 3′-r(CUCUCUUUUCUC)	[R_P]	50	32	50 (85)	35 (77)
	[S_P]	25	25	25 (28)	25 (27)
4 5′-d(AAGAGAAGAGAG)	[PO]	ND	ND	38	38
4W 3′-r(UUCUCUUCUCUC)	[R_P]	(60, 83)*	ND	34, 54	34
5 5′-d(GAGGAAAAAGAG)	[PO]	33	33	33	33
5W 3′-r(CUCCUUUUUCUC)	[R_P]	28	28	28	27
	[S_P]	25	25	25	24
5H 5′-r(CUCCUUUUUCUC)					
5 5′-d(GAGGAAAAAGAG)	[R_P]	ND	ND	(60)†	(54)
5W 3′-r(CUCCUUUUUCUC)					
6 5′-d(GAGAGGAAAGAG)	[PO]	42	42	42	42
6W 3′-r(CUCUCCUUUCUC)	[R_P]	37	37	37 (73)†	37
	[S_P]	34	34	34	34
7H 5′-r(CUCCUUUCUCUC)	[PO]	–	–	(43)‡	–
7 5′-d(GAGGAAAGAGAG)	[R_P]	–	–	(66,91)‡	–
7W 3′-r(CUCCUUUCUCUC)					

Buffer 10 mM Tris-HCl, 100 mM NaCl, 10 mM $MgCl_2$, pH 7.4. Temperature gradient 0.2°C/min. Data in parentheses were obtained for (2′-OMe)-RNA template.

*Watson-Crick strand 2′-OMe-RNA,

†Watson-Crick strand, 2′-OH; Hoogsteen strand, 2′-OMe-RNA.

‡Watson-Crick and Hoogsteen strands, 2′-OMe-RNA.

complex with U_{12} melts at 7°C. Also, the mixing curve for the samples equilibrated at 3°C confirmed the formation of a duplex. All these observations are consistent with the formation of the triplex U_{12}/[R_P-PS]-dA_{12}/U_{12}. Notably, the complex [S_P-PS]-dA_{12}/U_{12} has the melting temperature of 18°C, which is lower than that for dA_{12}/U_{12}.

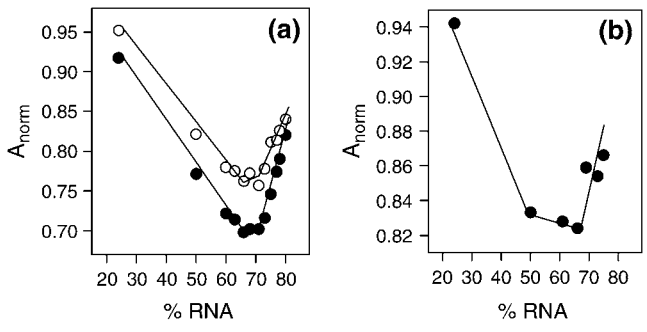

FIGURE 1 Normalized UV absorption for mixing of DNA and complementary RNA strands. (*a*) [R_P-PS]-dA_{12} (**1**) at 10°C (●) and 25°C (○); (*b*) [R_P-PS]-d(GAGGAAAAAGAG) (**5**) at 10°C.

Studies on the complexes of DNA with Watson-Crick complementary RNA strands

It was interesting to check whether 2′-OMe analog of the U_{12} template can form analogous stable structure as it is known that it adopts a conformation very similar to that for natural RNA (15). In melting experiments for [R_P-PS]-dA_{12}/(2′-OMe)-U_{12} mixed at 1:1 and 1:2 molar ratio, we found melting temperatures of 46°C and 53°C (Table 1, data in parentheses), respectively, i.e., higher than for the complex [R_P-PS]-dA_{12}/U_{12}.

In a second set of experiments, we compared the thermal stability of the complexes of [R_P-PS]-, [Mix-PS]- and [PO]-dA_n with (2′-OMe)-U_n (1:2 molar ratio) as a function of length n of oligomers (Fig. 3). We found that [R_P-PS]-oligo as short as [R_P-PS]-dA_6 with two molar equivalents of (2′-OMe)-U_6 strands, forms a complex with a T_m of 26°C, which is close to the T_m for a complex of dA_{10} with (2′-OMe)-U_{10}. Notably, for given length of oligonucleotides ($8 < n < 12$) the observed T_m values for [Mix-PS]-dA_n/(2′-OMe)-U_n are higher than for their dA_n/(2′-OMe)-U_n counterparts. These data establish the strength of the interactions stabilizing that unique triplex structure.

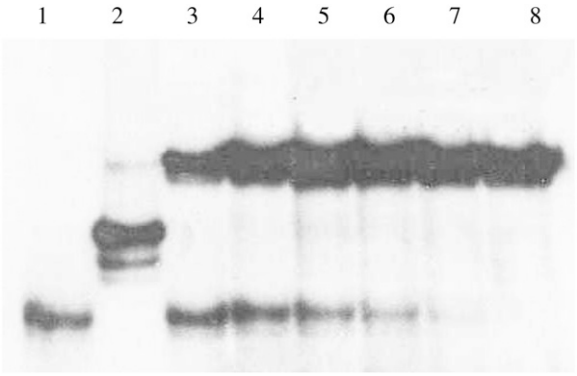

FIGURE 2 PAGE analysis of complexes [R_P-PS]-dA_{12}/U_{12} at different molar ratio. 20% polyacrylamide gel; 5 mM $MgCl_2$ in 89mM Tris-borate buffer and in the gel, temperature 8°C. (*Lane 1*) 5′-*O*-[$^{32}PO_3$]-[R_P-PS]-dA_{12}, (*lane 2*) 5′-*O*-[$^{32}PO_3$]-U_{12}, (*lanes 3–8*) 5′-*O*-[$^{32}PO_3$]-[R_P-PS]-dA_{12}/U_{12} ratio 2:1, 1:1, 1:1.5, 1:2, 1:2.5, and 1:3, respectively.

To identify other factors important for the formation of stable higher-order structures, five stereodefined R_P and S_P pairs of homopurine PS-dodecamers **2–6** (the numbering of compounds is given in Table 1) were synthesized, as well as their nonmodified precursors [PO]-**2-6** and Watson-Crick complementary oligoribonucleotides (**2W–6W**, Table 1). For complexes of [PO]-**2-6** with corresponding oligoribonucleotides **2W–6W** mixed at pH 7.4, the T_m values of 26–42°C were found, regardless of molar ratio (1:1 or 1:2; see Table l). The T_m values for the complexes consisting of PS-DNA and RNA strands mixed at neutral conditions showed that at the both relative concentrations [R_P-PS]-**2**, **-3** and **-4** form structures by 28°, 17°, and 16°C, respectively, more stable than their [PO]-counterparts. In melting/association experiments for complexes [R_P-PS]-**2/2W**, [R_P-PS]-**3/3W** and [R_P-PS]-**4/4W**, a hysteresis, i.e., the difference (15–20°C) between the melting temperature (T_m) and association temperature (T_a), was observed.

Although, formally, at pH 7.4 the protonation of cytosines in the third strand is uncertain (pKa 4.6 was found for free cytosine at 25°C) and the network of Hoogsteen hydrogen

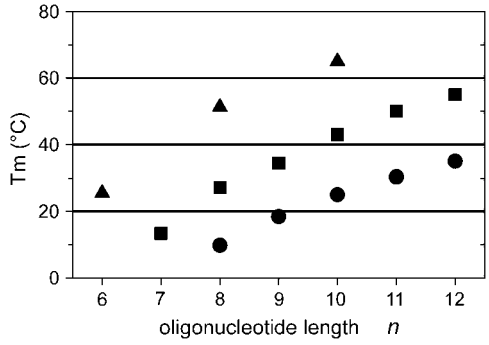

FIGURE 3 Melting temperatures for complexes of [PO]-dA_n (*circles*), [Mix-PS]-dA_n (*squares*), and [R_P-PS]-dA_n (*triangles*) mixed with two molar equivalents of (2′-OMe)-U_n as a function of oligonucleotide length *n*. Buffer: 10 mM $MgCl_2$, 10 mM Tris-Cl, pH 7.4, 100 mM NaCl.

bonds may be incomplete, NMR studies have been reported, showing that in a Py/Pu/Py DNA parallel triplex the cytosines involved in Hoogsteen basepairing remain protonated at pH 7.2 (30). Obviously, acidic conditions should stabilize the triplex structure. We observed such an enhancement as for oligomer [R_P-PS]-d(GAGAGAAAAGAG) (**3**) mixed with the oligoribonucleotide **3W** at pH 5.3 (1:2 molar ratio, five C-G-C^+ triplets) as the corresponding melting and association curves showed $T_m = 72°C$ and $T_a = 41°C$, compared to 50° and 35°C, respectively, at pH 7.3.

The complexes of unsymmetrical oligomers [R_P-PS]-d(GAGGAAAAAGAG) and [R_P-PS]-d(GAGAGGAAAGAG) with corresponding **5W** and **6W**, respectively, are by 5°C less stable than [PO]-**5/5W** and [PO]-**6/6W** and the lack of hysteresis indicates the duplex structure. The [S_P-PS]-oligomers analyzed form duplexes of lowest stability (T_m values of 18–34°C, no hysteresis). Thus, we conclude that the unusually high thermal stability of certain complexes of PS-DNA/RNA must be related to the sequence of the PS-oligo and to the presence of phosphorothioate linkages of R_P configuration.

The UV and PAGE monitored mixing experiments showed that at 10 and 25°C at neutrality (pH 7.4), [R_P-PS]-d(GAGAAAAAAGAG) ([R_P-PS]-**2**) and [R_P-PS]-d(GAGAGAAAAGAG) ([R_P-PS]-**3**) form a triplex structure with corresponding **2W** and **3W**. The corresponding mixing curve for oligomer [R_P-PS]-**3** titrated with the 2′-OMe analog of the oligoribonucleotide **3W** at 25°C also indicates formation of the triplex. Notably, the absence of a breakpoint at a 1:1 ratio suggests preferential formation of the triplexes (in equilibrium with the unbound PS-DNA strands), without detectable contribution of double-stranded species. This suggestion is confirmed by analysis of the FTIR spectra in the region 700–1000 cm^{-1} where bands characteristic for the furanose ring are present (31). When PS-oligo and complementary RNA were mixed at a 1:1 molar ratio, the bands at 858 and 877 cm^{-1}, indicating the A-conformation, are present. The overall A-conformation for [R_P-PS]-DNA/RNA duplexes has been reported in the literature (32–36). Interestingly, there are also three intensive bands at 818, 827, and 836 cm^{-1}, which are considered a strong indicator of S-type sugar conformation. Although these three bands may be attributed to multiple conformations of the deoxyribose moieties in the PS-DNA/RNA heteroduplexes (33), it is also possible that they reflect the presence of unbound PS-DNA oligomer existing in the B-form. The latter explanation is supported by observation that when both components were mixed at a 1:2 molar ratio, the bands for the A-conformation are present, whereas those for the B-form are of very low intensity. It must be emphasized that a mixing curve for [R_P-PS]-**5** recorded at 10°C confirmed the presence of a triplex structure, but, contrary to the mixing curves for [R_P-PS]-**1–3** mixed with corresponding **1W–3W**, the breakpoint at a 1:1 ratio was also observed (Fig. 1 *b*). This suggests low thermodynamic stability of this particular triplex.

Polarity of strands in the triplex: selection of model compounds and thermal stability studies

For all the analyzed sequences **1**–**6**, an antiparallel orientation of the Hoogsteen strand with respect to the homopurine core gives triplexes without any mismatches (e.g., structure **I**, Scheme 1) and, consequently, the formation of the triplexes should not depend on symmetry of the homopurine sequences. With the opposite orientation of the Hoogsteen strand, the mismatch-free parallel triplexes will be formed by the symmetrical, palindromic oligomers **1** and **2** (not shown). By contrast, the topological analysis of the possible Py/Pu/Py triple helices formed by the asymmetrical [R_P-PS]-**3** and [R_P-PS]-**4** clearly indicates that parallel orientation of the third strand would result either in two mismatches inside the sequence at the Hoogsteen side, marked with underlined letters, (structure **II**, Scheme 1) or in complementary but attenuated 10-nucleotide tracks (structures **III** or **IV**). It should be noticed that these complementarity imperfections correlate well with T_m values of 50 and 54°C compared to 54°C for the palindromic [R_P-PS]-**2/2W**, because **3** and **4** have one dG residue more than **2** and one might expect slightly higher thermal stability for their complexes.

Scheme 1

Structure **I** is an antiparallel triplex; structures **II–X** are parallel triplexes. Antiparallel and parallel Hoogsteen strands are depicted in bold and italics, respectively.

3W **3′-CUCUCUUUUCUC-5′**
3 5′-GAGAGAAAAGAG-3′
3W 3′-CUCUCUUUUCUC-5′
I

3W *5′-CUCUUUUCUCUC-3′*
3 5′-GAGAGAAAAGAG-3′
3W 3′-CUCUCUUUUCUC-5′
III

5W *5′-CUCUUUUUCCUC-3′*
5 5′-GAGGAAAAAGAG-3′
5W 3′-CUCCUUUUUCUC-5′
V

6W *5′-CUCUUUCCUCUC-3′*
6 5′-GAGAGGAAAGAG-3′
6W 3′-CUCUCCUUUCUC-5′
VII

5H *5′-CUCCUUUUUCUC-3′*
5 5′-GAGGAAAAAGAG-3′
5W 3′-CUCCUUUUUCUC-5′
IX

3W *5′-CUCUUUUCUCUC-3′*
3 5′-GAGAGAAAAGAG-3′
3W 3′-CUCUCUUUUCUC-5′
II

4W *5′-CUCUCUUCUCUU-3′*
4 5′-AAGAGAAGAGAG-3′
4W 3′-UUCUCUUCUCUC-5′
IV

5W *5′-CUCUUUUUCCUC-3′*
5 5′-GAGGAAAAAGAG-3
5W 3′-CUCUCUUUUCUC-5′
VI

6W *5′-CUCUUUCCUCUC-3′*
6 5′-GAGAGGAAAGAG-3′
6W 3′-CUCUCCUUUCUC-5′
VIII

6H *5′-CUCUCCUUUCUC-3′*
6 5′-GAGAGGAAAGAG-3′
6W 3′-CUCUCCUUUCUC-5′
X

For oligomers **5** and **6** the longest possible segments of undisturbed complementarity would be much shorter—only 4, 7, 5, and 3 nucleotides in complexes **V**–**VIII**, respectively. Undoubtedly, the length of possible complementary tracks should be important for overall stabilization of the triplex. Comparing this structural analysis with the observed relative stability (T_m values of 28 and 37°C for [R_P-PS]-**5/5W** and [R_P-PS]-**6/6W**, respectively), we are obliged to conclude that the triplex under investigation has parallel Hoogsteen and homopurine strands. To prove this hypothesis, two other (2′-OMe)-RNA templates 5′-r(CUCCUUUUUCUC)-3′ (**5H**) and 5′-r(CUCUCCUUUCUC)-3′ (**6H**) were synthesized and used in melting experiments. It was assumed that they should be able to hybridize with corresponding [R_P-PS]-**5/5W** and [R_P-PS]-**6/6W** duplexes to form the mismatch-free triplexes **IX** and **X** (see Scheme 1), giving rise to remarkable increase of melting temperature. For the complex [R_P-PS]-**5/5W** (the strands mixed at 1:1 and 1:2 ratio) the only transition observed on a corresponding melting curve was that at 28°C (with no hysteresis). In a melting experiment, where the oligomer [R_P-PS]-d(GAGGAAAAAGAG) (**5**) was mixed with equimolar amounts of **5W** and **5H** (Fig. 4), the T_m of 60°C and T_a of 54°C (a hysteresis of 6°) were found (pH 7.4), and the triplex structure was confirmed by the corresponding mixing curve. Even stronger enhancement of thermal stability ($T_m = 73$°C) was found for equimolar mixture of [R_P-PS]-d(GAGAGGAAAGAG) (**6**), **6W** and **6H**. Thus, these experiments further confirmed the parallel orientation of the Hoogsteen and homopurine strands in the triplexes under investigation.

Polarity of strands: fluorescence quenching studies

Additional proof of the parallel orientation was sought from fluorescence quenching studies. To that end, we synthesized a set of oligomers, consisting of d(GAGGAAAGAGAG) ([PO]-**7**), [R_P-PS]-d(GAGGAAAGAGAG) ([R_P-PS]-**7**), and [R_P-PS]- BHQ_{PS}d(GAGGAAAGAGAG) ([R_P-PS]-**7B**) labeled at the 5′-end with a dark quencher acceptor (black hole quencher (BHQ)). As RNA templates we used 5′-(2′-OMe)-CUCUCUUUCCUC (**7W**) complementary to **7** according to Watson-Crick pairing, and three 2′-OMe-RNA oligomers complementary to **7** according to Hoogsteen pairing, namely 5′-(2′-OMe)-CUCCUUUCUCUC (**7H**), 5′-Fl-(2′-OMe)-CUCCUUUCUCUC (**7Ha**), and 5′-(2′-OMe)-CUCCUUUCUCUC-Fl (**7Hb**); the two latter labeled with a fluorescein

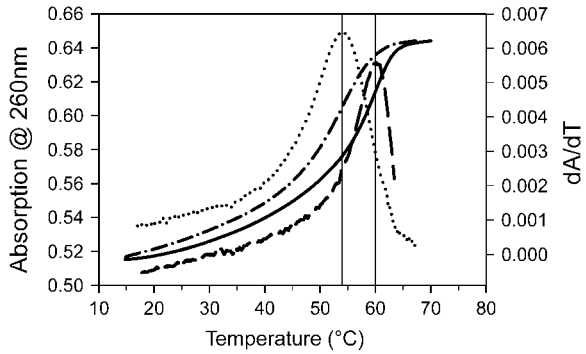

FIGURE 4 Melting (*solid line*) and association (*dash-dotted line*) curves for a complex 5′-(2′-OMe)-r(CUCCUUUUUCUC)-3′/[R_P-PS]-d(GAGGAAAAAGAG)/3′- CUCCUUUUUCUC-5′ (**5H**/[R_P-PS]-**5/5W**) and plots of dA/dT derivatives (*dashed* and *dotted lines*, respectively). Buffer: 10 mM Tris-HCl, 100 mM NaCl, 10 mM $MgCl_2$, pH 7.4.

donor (Fl) at the 5′- and 3′-end, respectively. The dodecameric sequence **7** is as much ''nonpalindromic'' as possible and was selected to assure the highest possible selectivity of association of DNA oligomers **7** with the corresponding Watson-Crick and Hoogsteen RNA templates. When **7Ha** or **7Hb** were mixed with **7W** and BHQ-labeled [R_P-PS]-**7B**, they were expected to form the specific complexes **XI** or **XII**, respectively (see Scheme 2). Because of the shorter distance between the BHQ and Fl moieties in **XI** compared to **XII**, stronger quenching of fluorescence should be observed.

Scheme 2

7Ha	5′-Fl-CUCCUUUCUCUC	**7Hb**	5′-CUCCUUUCUCUC-Fl
7B	5′-BHQ$_{PS}$GAGGAAAGAGAG	**7B**	5′BHQ$_{PS}$GAGGAAAGAGAG
7W	3′-CUCCUUUCUCUC	**7W**	3′-CUCCUUUCUCUC
	XI		XII

For the measurement of the initial fluorescein emission, i.e., in the absence of the [R_P-PS]-**7B** strand carrying the fluorescence quencher, the oligomers **7W** and either **7Ha** or **7Hb** were mixed at 2 μM concentration each, in a total volume of 1.0 mL. For the mixtures **7W/7Ha** and **7W/7Hb** (at room temperature) fluorescence intensities of 705 and 470 a.u., respectively, were measured (Fig. 5). These values remained virtually unchanged over 30 min observation. Then, aliquots (12 μL) of a solution containing the required amount of [R_P-PS]-BHQ$_{PS}$d(GAGGAAAGAGAG) were rapidly added ($\sim$90 s) to each sample (the 12-μL volume increase makes the dilution effect negligible), followed by thorough mixing, and the fluorescence decays were immediately monitored over time. The measurements revealed (Fig. 5) that at 25°C strand association occurred rather rapidly and the fluorescence intensities for both **XI** and **XII** reached a plateau within $<$6 min. Notably, the final fluorescence for **XI** was twofold lower than for **XII** (142 and 375 a.u., respectively), so the fluorescence intensities decreased by 80% and 21%, respectively. These data show that BHQ and Fl moieties are much closer in **XI** than in **XII**, which confirms the parallel orientation of the [R_P-PS]-**7B** and **7Ha** strands.

It must be pointed out that for the mixture **7W**/[R_P-PS]-**7**/**7H** (pH 7.4) the melting temperature of 91°C was found by UV spectroscopy. Thus, our attempts at fluorescence monitored thermal dissociation of **XI** and **XII**, which for technical reasons had to stop at 95°C, were only partially successful. Nonetheless, because the fluorescence intensity of the fluorescein moiety significantly and steadily decreases with increasing temperature (Fig. 6, mixture of 5′-CUCUCUUUCCUC-3′ and 5′-CUCCUUUCUCUC-Fl-3′, **7W**/**7Hb**, *dots*), we were able to observe slight increase of fluorescence for **XI** above 55°C (*triangles*), presumably resulting from partial dissociation of the complex **XI** below the melting point. This effect remained undetected in the case of **XII** (*crosses*), where quenching was much less effective, so the fluorescence enhancement upon dissociation was rather small. These results indicate that the [R_P-PS]-BHQ$_{PS}$d(GAGGAAAGAGAG) and 5′-Fl-CUCCUUUCUCUC remain associated up to 60°C and dissociate at higher temperatures. Although we were unable to continue measurement beyond 95°C, fluorescence intensities observed for both complexes **XI** and **XII** at 95°C are virtually identical to that for the mixture **7W/7Hb** and indicate the presence of free, unassociated strands.

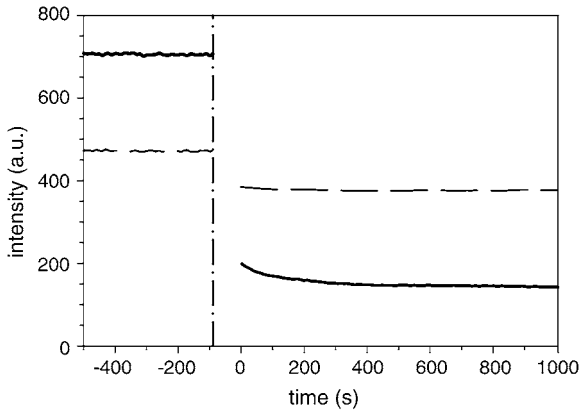

FIGURE 5 Initial fluorescence intensities and fluorescence decay for **XI** (*solid lines*) and **XII** (*dashed lines*). Vertical dash-dotted line indicates addition of [R_P-PS]-BHQ$_{PS}$d(GAGGAAAGAGAG). Parameters: excitation at 446 nm, emission detected at 516 nm, excitation and emission slits 5 nm, temperature 25°C, 12 data points per minute.

Possible mechanism of stabilization of the triplexes

These data show that the sulfur atoms of the internucleotide phosphorothioate linkages in [R_P] diastereomers of

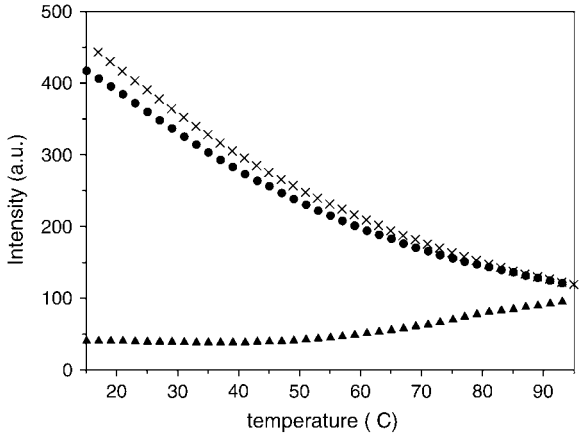

FIGURE 6 Fluorescence intensities at 516 nm for a mixture of 5′-CUCUCUUUCCUC-3′ and 5′-CUCCUUUCUCUC-Fl-3′ (**7W/7HB**, *dots*), **XI** (*triangles*), and **XII** (*crosses*) in melting experiments. Parameters: temperature gradient 1°C/min, data point collected at 1°C and presented at 2°C increment, excitation at 446nm, excitation and emission slits 5 nm. Intensities given in arbitrary units.

PS-homopurine oligomers have to be involved in strong and specific interactions stabilizing the parallel triplex. In 1993, on the basis of molecular modeling, Hélène et al. proposed a mechanism for interactions stabilizing Py/Pu/Py parallel triplex having a central unmodified DNA strand and two RNA strands (5). Relevant calculations demonstrated that the distance of 1.93 Å between the pro-R_P oxygen atom of the internucleotide bond in the central strand of the triplex and the 2′-OH group of ribose in the third strand permits direct hydrogen bonding. However, as we have set out earlier, among others, [R_P-PS]-**3** forms a triplex (Tm = 85°C) with the 2′-OMe analog of **3W**, which has no 2′-OH group, i.e., the hydrogen bond donor required by Hélène's model. So we conclude that the 2′-OH group does not play a role in the observed stabilization.

In searching for possible explanations, we appreciate that the common structural feature of cytidine and uridine moieties is the presence of an oxygen in position-2 of the pyrimidine ring. Because only PS-DNA of R_P configuration is able to stabilize the triplex efficiently, we suggest that a water bridge between the sulfur atom of an R_P- phosphorothioate (carrying most of the negative charge in a phosphorothioate anion (37)) and the pyrimidine O^2 of the third strand may provide a strong stabilizing force. Although it is commonly accepted that a sulfur atom is a weaker acceptor of hydrogen bonds than an oxygen atom, a few reports in the literature indicate that despite the comparatively diffused character of the acceptor electron pair, ionized sulfur atom is able to form strong hydrogen bonds (21,38–41). To verify this hypothesis FTIR measurements were conducted. The spectra recorded for (2′-OMe)-U_{12} alone and mixed at 1:1 molar ratio with [PO]-dA_{12}, [Mix-PS]-dA_{12} or [R_P-PS]-dA_{12} do not support this proposed involvement of the R_P-sulfur atoms in stabilization, because there are no significant differences in the range 1000–1160 cm^{-1} reported for P–S^- vibrations (42). However, at frequencies in the range 1600–1750 cm^{-1}, characteristic for bands resulting from C=O stretches in uracil rings, there are interesting changes. In this region, $C^2{=}O^2$ and $C^4{=}O^4$ stretches in a single-stranded RNA molecule are assigned at higher (1698–1691 cm^{-1}) and lower (1677–1672 cm^{-1}) wavenumbers, respectively (31). It is also known, that the band for $C^4{=}O^4$ decreases in intensity upon duplex formation (43). For a single-stranded (2′-OMe)-U_{12}, we observed two bands at 1697 and 1682 cm^{-1} of almost equal intensity (Fig. 7, curve *D*). The latter band is ~40% reduced upon addition of [Mix-PS]-dA_{12} and even more reduced in the presence of [PO]-dA_{12}, where in both cases the formation of duplexes was observed (curves *B* and *C*, respectively). Also, for [R_P-PS]-dA_{12} mixed with (2′-OMe)-U_{12} the intensity of the band at 1697 cm^{-1} is significantly reduced (Fig. 7, curve *A*) indicating strong involvement of the carbonyl group $C^2{=}O^2$ of the uracil ring, supposedly in hydrogen bonding.

Work on a more precise molecular description of this phenomenon using x-ray crystallography and NMR methods is in progress. We believe that the elucidation of the factors responsible for such a significant stabilization of this proposed novel triple-helical structure, specifically involving the R_P-sulfur atoms of internucleotide phosphorothioate bonds, may lead to a better understanding of the biological function and mode of action of PS-oligos. Moreover, the search for RNA sequences being able to form triple-helix complexes with exogenously delivered PS-oligos may open a new way for structural rearrangement of RNA and, hence, inhibition of the translation process.

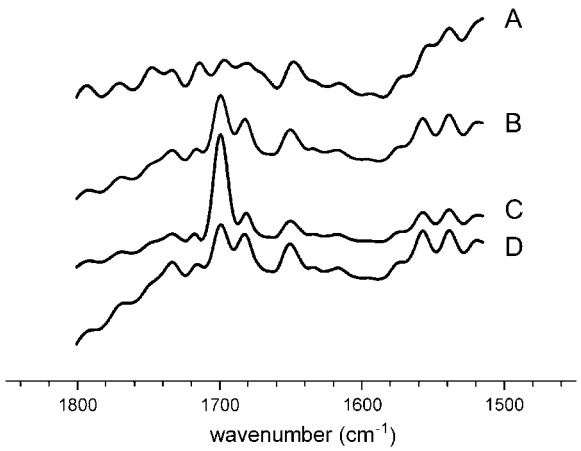

FIGURE 7 FTIR spectra (range 1500–1800 cm^{-1}) recorded for the following samples: (curve *A*) [R_P-PS]-dA_{12}/(2′-OMe)-U_{12}, (curve *B*) [Mix-PS]-dA_{12}/(2′-OMe)-U_{12}, (curve *C*) [PO]-dA_{12}/(2′-OMe)-U_{12}, (curve *D*) (2′-OMe)-U_{12}.

SUPPLEMENTARY MATERIAL

An online supplement to this article can be found by visiting BJ Online at http://www.biophysj.org. Supporting information available includes FT-IR spectra for [R_P-PS]-dA_{12}/U_{12} mixed at 1:1 and 1:2 molar ratio and discussion on the ability of an ionized sulfur atom in a phosphorothioate moiety to form strong hydrogen bonds.

Words of gratitude are directed to Dr. George M. Blackburn for critical reading of the manuscript and valuable suggestions, and to Dr. Eric Westhoff and Dr. Grzegorz Bujacz for their help in our so far unsuccessful attempts at crystallization of model triplexes for x-ray analysis. Authors thank Mrs. Genowefa Nowak for the synthesis of DNA and RNA oligomers. Kind help of Dr. Maria Bryszewska and Dr. Barbara Klajnert in initial fluorescence measurements is gratefully acknowledged.

This work was financially assisted by the State Committee for Scientific Research (Ministry of Science and Information, Poland; grants Z-KBN K005/T09 and 3T09A 059 28 to W.J.S and grant 3 T09A 072 26 to P.G). The CD6 dichrograph has been financed by the BIMOL program of the Polish Science Foundation.

REFERENCES

1. Felsenfeld, G., V. Davies, and A. Rich. 1957. Formation of a three-stranded polynucleotide molecule. *J. Am. Chem. Soc.* 79:2023–2024.

2. Hélène, C. 1993. In Antisense Research and Application. S. T. Crook, and B. Lebleu, editors. CRC Press Inc. Boca Raton, Ann Arbor, London, Tokyo. 375–385 and references cited therein.
3. Roberts, R. W., and D. M. Crothers. 1992. Stability and properties of double and triple helices: dramatic effects of RNA or DNA backbone composition. *Science*. 258:1463–1466.
4. Han, H., and P. B. Dervan. 1993. Sequence-specific recognition of double helical RNA and RNA·DNA by triple helix formation. *Proc. Natl. Acad. Sci. USA*. 90:3806–3810.
5. Escudé, C., J.-C. François, J.-S. Sun, G. Ott, M. Sprinzl, T. Garestier, and C. Hélène. 1993. Stability of triple helices containing RNA and DNA strands: experimental and molecular modeling studies. *Nucleic Acids Res*. 21:5547–5553.
6. Strobel, S. A., L. A. Doucette-Stamm, L. Riba, D. E. Housman, and P. B. Dervan. 1991. Site-specific cleavage of human chromosome 4 mediated by triple helix. *Science*. 254:1639–1642.
7. Maher III, L. J., P. B. Dervan, and B. Wold. 1992. Analysis of promoter-specific repression by triple-helical DNA complexes in a eukaryotic cell-free transcription system. *Biochemistry*. 31:70–81.
8. Mayfield, C., M. Squibb, and D. Miller. 1994. Inhibition of nuclear protein binding to the human Ki-ras promoter by triplex-forming oligonucleotides. *Biochemistry*. 33:3358–3363.
9. Hobbs, C. A., and K. Yoon. 1994. Differential regulation of gene expression in vivo by triple helix-forming oligonucleotides as detected by a reporter enzyme. *Antisense Res. Dev*. 4:1–8.
10. Verma, S., and F. Eckstein. 1998. Modified oligonucleotides: synthesis and strategy for users. *Annu. Rev. Biochem*. 67:99–134.
11. Dagle, J. M., J. L. Littig, L. B. Sutherland, and D. L. Weeks. 2000. Targeted elimination of zygotic messages in *Xenopus laevis* embryos by modified oligonucleotides possessing terminal cationic linkages. *Nucleic Acids Res*. 28:2153–2157.
12. Nielsen, P. E., and M. Egholm. 1999. An introduction to peptide nucleic acid. *Curr. Issues Mol. Biol*. 1:89–104.
13. Summerton, J. 1999. Morpholino antisense oligomers: the case for a RNase H-independent structural type. *Biochim. Biophys. Acta*. 1489: 141–158.
14. Boczkowska, M., P. Guga, and W. J. Stec. 2002. Stereodefined phosphorothioate analogues of DNA: relative thermodynamic stability of the model PS-DNA/DNA and PS-DNA/RNA complexes. *Biochemistry*. 41:12483–12487.
15. Freier, S. M., and K. H. Altmann. 1997. The ups and downs of nucleic acid duplex stability: structure-stability studies on chemically modified DNA:RNA duplexes. *Nucleic Acids Res*. 25:4429–4443.
16. Stec, W. J., and A. Wilk. 1994. Stereocontrolled synthesis of oligo (nucleoside phosphorothioate)s. *Angew. Chem. Int. Ed. Engl.* 33:709–722.
17. Wilk, A., and W. J. Stec. 1995. Analysis of oligo(deoxynucleoside phosphorothioate)s and their diastereomeric composition. *Nucleic Acids Res.* 23:530–534.
18. Guga, P. M., Koziołkiewicz, A. Okruszek, and W. J. Stec. Oligo(nucleoside phosphorothioate)s. 1998. *In* Applied Antisense Oligonucleotide Technology. C. A. Stein and A. M. Krieg, editors. Wiley-Liss, New York. 23–50.
19. Stec, W. J., B. Karwowski, M. Boczkowska, P. Guga, M. Koziołkiewicz, M. Sochacki, M. Wieczorek, and J. Błaszczyk. 1998. Deoxyribonucleoside 3′-*O*-(2-thio- and 3′-*O*-(2-oxo-′′spiro′′-4.4-pentamethylene-1.3.2-oxathiaphospholanes): monomers for stereocontrolled synthesis of oligo(nucleoside phosphorothioate)s and chimeric PS/PO oligonucleotides. *J. Am. Chem. Soc*. 120:7156–7167.
20. Guga, P., and W. J. Stec. 2003. Synthesis of phosphorothioate oligonucleotides with stereodefined phosphrothioate linkages. *In* Current Protocols in Nucleic Acid Chemistry. S. L. Beaucage, D. E. Bergstrom, G. D. Glick, and R. A. Jones, editors. John Wiley and Sons, Hoboken, NJ. 4.17.1–4.17.28.
21. Boczkowska, M., P. Guga, B. Karwowski, and A. Maciaszek. 2000. Effect of P-chirality of internucleotide bonds on B-Z conversion of stereodefined self-complementary phosphorothioate oligonucleotides of the [PS]-d$(CG)_4$ and [PS]-d$(GC)_4$ series. *Biochemistry*. 39:11057–11064.
22. Kim, S.-G., S. Tsukahara, S. Yoyama, and H. Takaku. 1992. The influence of oligodeoxyribonucleotide phosphorothioate pyrimidine strands on triplex formation. *FEBS Lett*. 314:29–32.
23. Xodo, L., M. Alunni-Fabroni, G. Manzini, and F. Quadrifoglio. 1994. Pyrimidine phosphorothioate oligonucleotides form triple-stranded helices and promote transcription inhibition. *Nucleic Acids Res*. 22:3322–3330.
24. Hacia, J. G., B. Wold, and P. B. Dervan. 1994. Phosphorothioate oligonucleotide-directed triple helix formation. *Biochemistry*. 33:5367–5369.
25. Joseph, J., J. C. Kandala, D. Veerapanane, K. T. Weber, and R. V. Guntaka. 1997. Antiparallel polypurine phosphorothioate oligonucleotides form stable triplexes with the rat α1(I) collagen gene promoter and inhibit transcription in cultured rat fibroblasts. *Nucleic Acids Res.* 25:2182–2188.
26. Latimer, L. J., P. K. Hampel, and J. S. Lee. 1989. Synthetic repeating sequence DNAs containing phosphorothioates: nuclease sensitivity and triplex formation. *Nucleic Acids Res.* 17:1549–1561.
27. Stec, W. J., A. Grajkowski, B. Karwowski, A. Kobylańska, M. Koziołkiewicz, K. Misiura, A. Okruszek, A. Wilk, P. Guga, and M. Boczkowska. 1995. Diastereomers of nucleoside 3′-*O*-(2-thio-1,3,2-oxathia(selena)phospholanes): building blocks for stereocontrolled synthesis of oligo(nucleoside phosphorothioate)s. *J. Am. Chem. Soc*. 117:12019–12029.
28. Brown, T., C. E. Pritchard, G. Turner, and S. A. Salisbury. 1989. A new base-stable linker for solid-phase oligonucleotide synthesis. *J. Chem. Soc. Chem. Commun*.891–893.
29. Brown, T., and D. J. S. Brown. 1991. Modern machine-aided methods of oligodeoxyribonucleotide synthesis. *In* Oligonucleotides and Analogues: A Practical Approach. F. Eckstein, editor. IRL Press, Oxford, UK. 20.
30. Bhaumik, S. R., K. V. R. Chary, G. Govil, K. Liu, and H. T. Miles. 1998. A novel palindromic triple-stranded structure formed by homopyrimidine dodecamer d-CTTCTCCTCTTC and homopurine hexamer d-GAAGAG. *Nucleic Acids Res.* 26:2981–2988.
31. Banyay, M., M. Sarkar, and A. Graslund. 2003. A library of IR bands of nucleic acids in solution. *Biophys. Chem*. 104:477–488.
32. González, C., W. Stec, A. Kobylańska, R. I. Hogrefe, M. Reynolds, and T. L. James. 1994. Structural study of a DNA·RNA hybrid duplex with a chiral phosphorothioate moiety by NMR: extraction of distance and torsion angle constraints and imino proton exchange rates. *Biochemistry*. 33:11062–11072.
33. González, C., W. J. Stec, M. A. Reynolds, and T. L. James. 1995. Structure and dynamics of a DNA·RNA hybrid duplex with a chiral phosphorothioate moiety: NMR and molecular dynamics with conventional and time-averaged restraints. *Biochemistry*. 34:4969–4982.
34. Bachelin, M., G. Hessler, G. Kurz, J. G. Hacia, P. B. Dervan, and H. Kessler. 1998. Structure of a stereoregular phosphorothioate DNA/RNA duplex. *Nat. Struct. Biol*. 5:271–276.
35. Furrer, P., T. M. Billeci, A. Donati, C. Kojima, B. Karwowski, A. Sierzchała, W. J. Stec, and T. L. James. 1999. Structural effect of complete [Rp]-phosphorothioate and phosphorodithioate substitutions in the DNA strand of a model antisense inhibitor-target RNA complex. *J. Mol. Biol*. 285:1609–1622.
36. Kanaori, K., Y. Tamura, T. Wada, M. Nishi, H. Kanehara, T. Morii, K. Tajima, and K. Makino. 1999. Structure and stability of the consecutive stereoregulated chiral phosphorothioate DNA duplex. *Biochemistry*. 38:16058–16066.
37. Frey, P. A., and R. D. Sammons. 1985. Bond order and charge localization in nucleoside phosphorothioates. *Science*. 228:541–545.
38. Boorman, P. M., X. Gao, and M. Parvez. 1992. X-ray structural characterization of a thiolate salt displaying a very strong S-H···S hydrogen bond. *J. Chem. Soc. Chem. Commun*.1656–1658.

39. Krebs, B. 1983. Thio- and seleno-compounds of main group elements: novel inorganic oligomers and polymers. *Angew. Chem. Int. Ed. Engl.* 22:113–134.

40. Mikołajczyk, M., J. Omelańczuk, W. S. Abdukakharov, A. Miller, M. W. Wieczorek, and J. Karolak-Wojciechowska. 1982. Synthesis of tetramethylammonium salt of 2-oxo-2-thio-1,3,2-oxazaphosphorinan and its crystal and molecule structure. *Tetrahedron.* 38:2183–2188.

41. Dertinger, D., L. S. Behlen, and O. C. Uhlenbeck. 2000. Using phosphorothioate-substituted RNA to investigate the thermodynamic role of phosphates in a sequence specific RNA-protein complex. *Biochemistry.* 39:55–63.

42. White, A. P., K. K. Reeves, E. Snyder, J. Farrell, J. W. Powell, V. Mohan, R. H. Griffey, and H. Sasmor. 1996. Hydration of single-stranded phosphodiester and phosphorothioate oligodeoxyribonucleotides. *Nucleic Acids Res.* 24:3261–3266.

43. Tsuboi, M. 1969. Application of infrared spectroscopy to structure studies of nucleic acids. *In* Applied Spectroscopy Reviews. E. G. J. Brame, editor. Dekker, New York. 45–90.